Environmental Science & Technology Letters

pubs.acs.org/journal/estlcu

Letter

Development of Electrospun Nanofibrous Filters for Controlling Coronavirus Aerosols

Hongchen Shen,[‖] Zhe Zhou,[‖] Haihuan Wang,[‖] Mengyang Zhang, Minghao Han, David P. Durkin, Danmeng Shuai,* and Yun Shen*

Cite This: *Environ. Sci. Technol. Lett.* 2021, 8, 545−550

Read Online

ACCESS | Metrics & More | Article Recommendations | Supporting Information

ABSTRACT: Airborne transmission of SARS-CoV-2 plays a critical role in spreading COVID-19. To protect public health, we designed and fabricated electrospun nanofibrous air filters that hold promise for applications in personal protective equipment (PPE) and the indoor environment. Due to ultrafine nanofibers (~300 nm), the electrospun air filters had a much smaller pore size in comparison to the surgical mask and cloth masks (a couple of micrometers versus tens to hundreds of micrometers). A coronavirus strain served as a SARS-CoV-2 surrogate and was used to generate aerosols for filtration efficiency tests, which can better represent SARS-CoV-2 in comparison to other agents used for aerosol generation in previous studies. The electrospun air filters showed excellent performance by capturing up to 99.9% of coronavirus aerosols, which outperformed many commercial face masks. In addition, we observed that the same electrospun air filter or face mask removed NaCl aerosols equivalently or less effectively in comparison to the coronavirus aerosols when both aerosols were generated from the same system. Our work paves a new avenue for advancing air filtration by developing electrospun nanofibrous air filters for controlling SARS-CoV-2 airborne transmission.

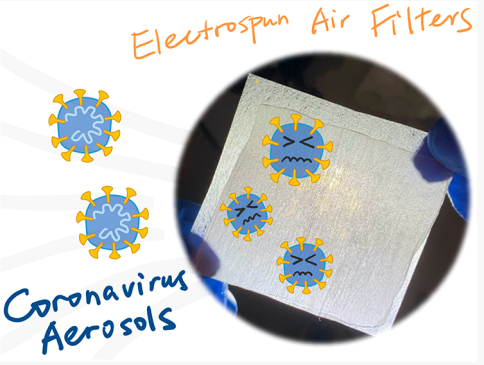

INTRODUCTION

Airborne transmission of SARS-CoV-2 has been recognized.[1,2] Virus-laden aerosols (<5 μm) can be suspended in the air for a long duration, accumulate in a closed environment, remain infectious,[3] and thus be involved in the short- and long-range transmission of airborne diseases. One accepted strategy to control SARS-CoV-2 airborne transmission is to wear face masks and respirators. However, cloth masks do not always have satisfactory aerosol removal efficiency, droplet repulsion, and/or breathability.[4] SARS-CoV-2 in the indoor environment can also potentially spread through heating, ventilation, and air conditioning (HVAC) systems.[5] However, most HVAC air filters used in residential, commercial, and industrial buildings do not capture airborne viruses.[6] Nanotechnology holds promise for developing effective, scalable, and affordable air filters for both mask/respirator and HVAC system applications.

Electrospinning is an emerging technology to synthesize nonwoven nanofibrous membranes that are ideal for air filtration.[7−11] Electrospun air filters have a reduced pore size (submicrometers to several micrometers) in comparison to conventional filters and thus enable the effective capture of small airborne particles.[12] The large porosity of electrospun air filters also reduces the air pressure drop or increases breathability.[13] More importantly, electrospinning is operated under a strong electric field (i.e., 1−5 kV cm^{-1}), and it produces filters with long-lasting retained charges that can significantly promote aerosol capture through electrostatic attraction.[14] Electrospun nanofibrous membranes have shown excellent performance for removing aerosols generated from polystyrene beads, NaCl, and bacteria.[13,15−19]

To date, many studies have evaluated the filtration efficiency of air filters and face masks by using surrogate aerosols instead of coronavirus aerosols.[13,15−21] However, it remains elusive whether the reported filtration performance can be used for coronavirus control because of property differences (e.g., size, density, surface charge, morphology, and chemical composition) between the surrogates and the coronavirus. Moreover, electrospun air filters for the capture of viral aerosols have not yet been reported. Murine hepatitis virus A59 (MHV-A59), a β-coronavirus with a diameter of ~85 nm[22] and in the same family as SARS-CoV-2, was selected for aerosol filtration. For the first time, we used coronavirus aerosols to challenge air filters and face masks and to evaluate their efficiency, and we

Received: May 3, 2021
Accepted: May 10, 2021
Published: May 17, 2021

https://doi.org/10.1021/acs.estlett.1c00337
Environ. Sci. Technol. Lett. 2021, 8, 545−550

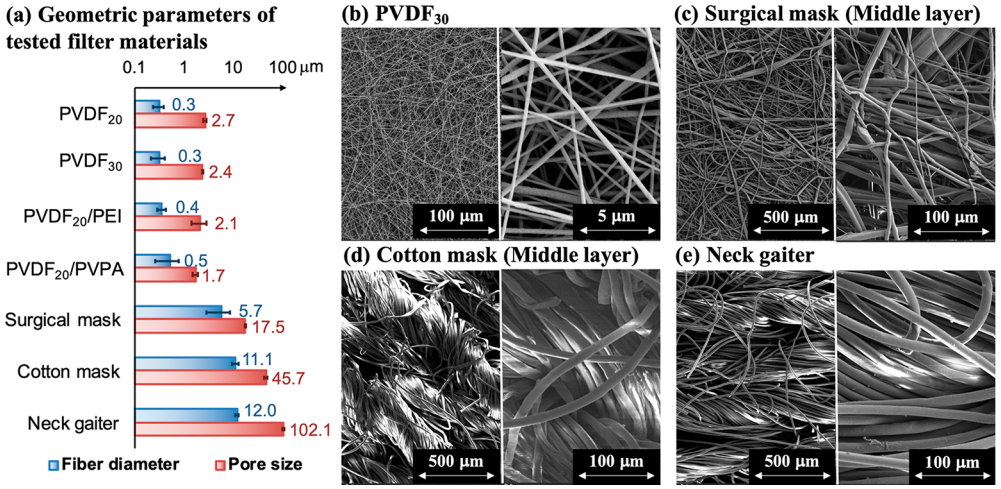

Figure 1. (a) Geometric parameters of tested filter materials and SEM of (b) $PVDF_{30}$, (c) surgical mask middle layer, (d) cotton mask middle layer, and (e) neck gaiter. The pore size here is the mean pore size measured by gas−liquid porometry. The error represents the standard deviation of the mean pore size measurements from triplicate samples for each filter. The largest and smallest pore sizes of the tested filter materials are included in Table S1.

developed electrospun nanofibrous air filters with a reduced pore size that can capture viral aerosols effectively.

MATERIALS AND METHODS

Fabrication of Electrospun Air Filters. We used a customized system[23] to electrospin 15 wt % polyvinylidene fluoride (PVDF, Arkema KYNAR 761) in *N*,*N*-dimethylformamide/acetone (7/3, v/v) onto a layer of polypropylene fabrics (PP, VWR 414004-680). The feeding rate of the working solution, electric field, and electrospinning duration were set at 0.6 mL h^{-1}, 1 kV cm^{-1}, and 20 or 30 min, respectively. The fabricated electrospun air filters were designated as $PVDF_{20}$ and $PVDF_{30}$, respectively. To promote virus removal efficiency by electrostatic attraction, a positively or negatively charged polyelectrolyte, i.e., poly(ethylenimine) (PEI) or poly(vinylphosphonic acid) (PVPA),[24] was coated onto $PVDF_{20}$ via soaking and drying, and the fabricated filters were denoted as $PVDF_{20}$/PEI and $PVDF_{20}$/PVPA, respectively.

Characterization of Electrospun Air Filters and Face Masks. A three-layer nonwoven surgical mask, a three-layer woven cotton mask, and a one-layer woven polyester neck gaiter were selected as representative commercial face masks. The fiber diameter of the electrospun air filters and the face masks were determined by scanning electron microscopy (SEM, FEI Teneo LV). The PEI or PVPA coating was characterized by attenuated total reflectance-Fourier transform infrared spectroscopy (ATR-FTIR, iS10 Nicolet Thermo). The mean flow pore size, largest pore size, and smallest pore size were examined by a gas liquid porometry method (POROLUX 100/200/500, shape factor of 0.715, APTCO Technologies LLC, Belgium). The pressure drop was determined with a face velocity of 5.3 cm s^{-1}.

Determination of Filtration Efficiency for Coronavirus and NaCl Aerosols. NaCl solution (0.1 M) and MHV-A59 in phosphate-buffered saline (PBS, ~10^8 gene copies mL^{-1}) were used for aerosolization and filtration tests. MHV-A59 was cultured in HeLa-mCC1a cells,[25] purified by centrifugal ultrafiltration (Nanosep, 300 kDa, Pall Laboratory), and diluted in PBS. Only for the aerosol size characterization were aerosols generated from PBS containing 100 nm polystyrene and 100 nm silica nanoparticles (00876-15, Polysciences; SISN100-25M, nanoComposix) to simulate MHV-A59 aerosols, owing to a similar particle/virion size and concentration as well as representative hydrophobicity of the nanoparticles.

The filtration efficiency was evaluated by a customized aerosolization setup (CH Technologies, Inc.; Figure S1). Specifically, the aerosols were generated by a high-output Blaustein atomizer (BLAM) with four jets, and a high-rate air flow (~1.5 L min^{-1}) sheared the liquid flow (15 mL h^{-1}) of the NaCl or MHV-A59 solution into aerosols. A single-pass atomization was applied to minimize virus damage during aerosolization. A portion of the aerosols with a controlled flow rate of 0.5 standard liter (tidal volume) per minute next passed through a fitted, 11.0 cm^2 air filter/face mask mounted on a stainless-steel holder and an impinger sequentially, and each filtration test (i.e., filter-on) was conducted for 30 min. The size distribution of aerosols that traveled to the filter holder before filtration was recorded by a Palas Promo 2000 instrument (detection limit of 200 nm to 10 μm) and reported as the number frequency. NaCl or MHV-A59 aerosols that penetrated through the filter/mask were retained by the impinger filled with ultrapure water or PBS (4 mL), respectively. Control experiments (i.e., filter-off) were conducted to quantify the NaCl or MHV-A59 aerosols collected in the impinger without an installed air filter/face mask. Each filter-on and filter-off experiment was conducted at least in duplicate, and the filtration efficiency, including mean, maximum, and minimum values, was calculated from the difference of the amount of the testing agent (NaCl or MHV-A59) in the impinger between filter-off and filter-on experiments over the amount of the testing agent in the impinger in the filter-off experiment (Text S1). PBS instead of water was used to suspend MHV-A59 because it simulated coronavirus aerosol generation under physiological conditions,[26,27] and solution matrices did not affect the aerosol filtration efficiency (Text S2).

NaCl and MHV-A59 were quantified by ion chromatography (Dionex ICS-1100) and a reverse transcription-quantitative polymerase chain reaction (RT-qPCR), respectively. Viral RNA was extracted by the Zymo Quick-RNA Viral

https://doi.org/10.1021/acs.estlett.1c00337
Environ. Sci. Technol. Lett. 2021, 8, 545−550

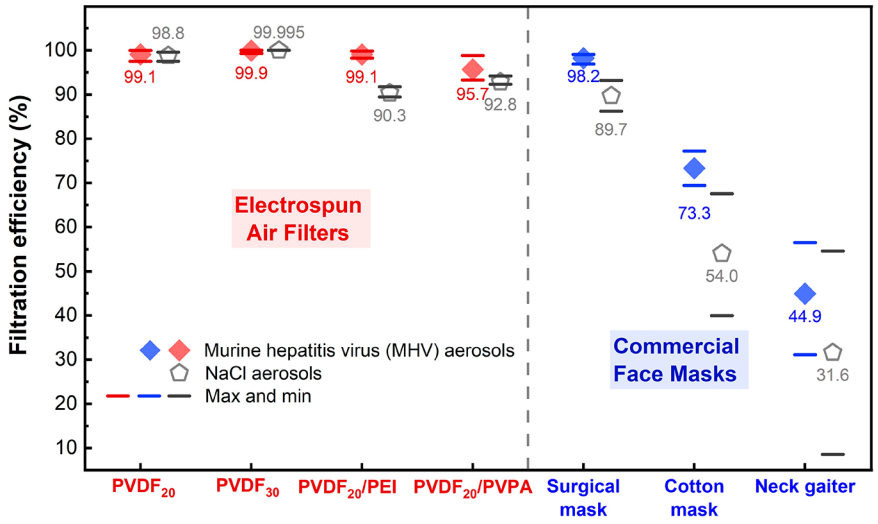

Figure 2. Aerosol filtration efficiency of electrospun air filters and commercial face masks. Aerosols generated from a coronavirus (MHV-A59) and NaCl were used for tests. Red and blue diamonds represent the average filtration efficiency of MHV-A59 aerosols by the electrospun air filters and the commercial face masks, respectively. Gray pentagons represent the average filtration efficiency of NaCl aerosols. Red, blue, and gray bars represent maximum and minimum values of the filtration efficiency in replicates.

Kit (R1035), and RT-qPCR was conducted using the TaqMan Fast Virus 1-Step Master Mix kit (Thermo Fisher Scientific Inc., 4444432). The primers, probe, and standard were designed on the basis of the literature.[28] Details of RT-qPCR quantification are included in Text S3.

Statistical Analysis. Student's t test was applied for the statistical comparison of the nanofiber diameter, pore size, and filtration efficiency of different air filters and face masks, which returned a p value. All p values <0.05 were considered statistically significant.

RESULTS AND DISCUSSION

Electrospun Air Filters Had Small Fiber Diameters and Pore Sizes. Electrospun PVDF air filters had much smaller fiber diameters and pore sizes in comparison to the commercial face masks (Figure 1 and Figure S2). The fiber diameters of $PVDF_{20}$, $PVDF_{30}$, $PVDF_{20}$/PEI, and $PVDF_{20}$/PVPA were in the range 0.2−1.3 μm. In comparison to $PVDF_{20}$, $PVDF_{30}$ showed a similar fiber diameter and pore size (both $p > 0.05$), but its increased thickness induced a slightly higher pressure drop (0.23 ± 0.00 versus 0.20 ± 0.00 inches of water column (inch wc)). FTIR characterization indicated the successful coating of PEI or PVPA onto the electrospun PVDF air filters (Figure S2). The fiber diameter of $PVDF_{20}$/PEI and $PVDF_{20}$/PVPA did not change in comparison with $PVDF_{20}$ (both $p > 0.05$). However, PEI and PVPA were observed to block pores in air filters. For $PVDF_{20}$/PVPA, its pores were partially blocked (Figure S3b), leading to a smaller pore size in comparison to $PVDF_{20}$ ($p = 0.006$). For $PVDF_{20}$/PEI, some pores, especially the small ones, were completely blocked (Figure S3c), but the mean pore size was comparable with that of $PVDF_{20}$ ($p = 0.27$). Both $PVDF_{20}$/PEI and $PVDF_{20}$/PVPA showed increased pressure drops of 1.19 ± 0.59 and 0.38 ± 0.04 inch wc, respectively, in comparison to $PVDF_{20}$.

Among the three commercial face masks, the middle layer of the surgical mask, which is the effective filtration medium, showed the smallest fiber diameter of 5.7 ± 2.8 μm, while the neck gaiter showed the largest fiber diameter of 12.0 ± 1.0 μm. A larger fiber diameter corresponded to a larger pore size: all of the electrospun filters had a mean pore size ≤2.7 μm, all of the commercial masks had a mean pore size ≥17.5 μm, and the largest mean pore size of 102.1 ± 4.4 μm was observed for the neck gaiter. The positive correlation between the filter fiber diameter and the pore size agreed with previous studies.[29] The filters with a larger fiber diameter and pore size showed a lower filtration efficiency for airborne particles.[30] Therefore, we expect that electrospun air filters would outperform the commercial face masks for removing airborne coronavirus particles. Due to a large pore size, the surgical mask, cotton mask, and neck gaiter had low pressure drops of 0.06 ± 0.01, 0.06 ± 0.01, and 0.01 ± 0.00 inch wc, respectively, and a negligible increase in the pressure drop was observed after filtration.

All the electrospun filters had an average filtration efficiency of ≥95.7%, while the commercial face masks showed an average filtration efficiency of 44.9% for the neck gaiter, 73.3% for the cotton mask, and 98.2% for the surgical mask, respectively (Figure 2). The aerosol removal efficiency indeed increased with the decrease in the mask pore size.[29,30] An increase in the electrospinning duration and thickness of the air filters enhanced coronavirus aerosol removal (99.9% and 99.1% for $PVDF_{30}$ and $PVDF_{20}$, respectively), though there was a marginal decrease in the pore size of $PVDF_{30}$ in comparison to $PVDF_{20}$. A polyelectrolyte coating did not promote electrospun air filters for removing coronavirus aerosols, and the average filtration efficiencies for $PVDF_{20}$/PEI and $PVDF_{20}$/PVPA were 99.1% and 95.7%, respectively. We speculate that coronavirus aerosol capture was dominated by interception, impaction, and diffusion, instead of the long-range force of electrostatic attraction, since the sizes of the aerosols and electrospun filter pores are close. The fact that the PVPA coating reduced the aerosol removal efficiency may indicate that coronavirus aerosols are negatively charged under the experimental conditions, and electrostatic repulsion might play a role in filtration. The PP fabrics for supporting the electrospun membrane removed a very limited amount of aerosols (0−30%), suggesting that the electrospun layer determined the performance of virus capture (Text S4). In comparison to the commercial face masks, the electrospun filters showed better reproducibility in measured filtration

https://doi.org/10.1021/acs.estlett.1c00337
Environ. Sci. Technol. Lett. 2021, 8, 545−550

efficiency, likely due to a more uniform pore size distribution (Table S1) and enhanced filtration performance.

To the best of our knowledge, our study is the first to evaluate the filtration efficiency of air filters/face masks by using coronavirus aerosols rather than surrogates. Bacteriophages have been used as the surrogates,[20,21] and a study revealed that the surgical mask removed 98.3−100% of MS2 aerosols.[20] However, MS2 is a nonenveloped virus with an average size of 27 nm, which is very different from SARS-CoV-2 with an envelope structure and a virion size of 50−200 nm.[31] In addition, that study only tested the filtration of aerosols of several micrometers (2.6 and 6.0 μm).[20] Aerosols with a size of 100−500 nm are the most penetrating for mechanical filters,[32,33] but filtration of viral aerosols with those sizes has not yet been studied. Inorganics have also been used as the surrogates, and filtration efficiencies of ∼88% and ∼63% were reported for removing 125 nm silica aerosols and 178 nm NaCl aerosols for the surgical mask, respectively.[4,34] However, these inorganic aerosols are even more different from the coronavirus aerosols in comparison to the bacteriophage aerosols. The MHV-A59 aerosols used in our study can best represent SARS-CoV-2 aerosols in filtration efficiency evaluation. Moreover, the size distribution of simulated MHV-A59 aerosols, generated from polystyrene and silica nanoparticles in PBS, highlighted that the most dominant aerosol size was 490−520 nm and 62−72% of the aerosols were <486 nm (Figure S4). The result indicated that the electrospun air filters could remove the most penetrating aerosols effectively.

Filtration Efficiency of NaCl Aerosols Is Equivalent to or Lower than That of Coronavirus Aerosols. The filtration efficiency of removing coronavirus and NaCl aerosols was compared for electrospun air filters and commercial face masks (Figure 2). For $PVDF_{20}$, $PVDF_{30}$, $PVDF_{20}$/PVPA, cotton mask, and neck gaiter, using MHV-A59 or NaCl aerosols did not lead to a significant difference in the filtration efficiency (all $p > 0.05$). The filtration efficiency of NaCl aerosols for $PVDF_{20}$/PEI and the surgical mask was significantly lower than that of MHV-A59 aerosols (p = 0.0008 and 0.04). The most dominant NaCl aerosol size was 420−450 nm, which was close to that of simulated MHV-A59 aerosols (490−520 nm). Some larger aerosol particles of 600 nm to 2 μm were observed in the NaCl aerosols but not for the simulated MHV-A59 aerosols (Figure S4). Larger aerosols beyond the most penetrating sizes are expected to be more easily removed in air filtration; surprisingly, our study observed that the filtration efficiency for NaCl aerosols was always statistically lower than or equal to that of coronavirus aerosols, which requires further investigation. Therefore, for the same tested air filter or face mask, NaCl aerosols were filtered equivalently or less effectively in comparison to coronavirus aerosols in our system, when the same aerosol generation system and the same operational conditions were applied. Since tests with pathogenic viral aerosols require high biosafety levels, NaCl aerosols are more easily handled for filtration tests and they are always used as a surrogate.[4,35−37] However, special attention should be paid to interpreting our results, because both NaCl and coronavirus aerosols may contain aerosol particles smaller than 200 nm, which could not be quantified by the Palas Promo 2000 instrument. In addition, both NaCl and coronavirus aerosols produced in our setup had a broad size range from hundreds of nanometers to a couple of micrometers, but the aerosol filtration efficiency should be compared for both aerosols with a narrow size range to evaluate the surrogate validity. Moreover, how the charge and size of coronavirus aerosols, the charge of filters, and other experimental conditions (e.g., flow rate of aerosols) affect the filtration efficiency of NaCl and coronavirus aerosols is unknown. Therefore, future work should explore these items to understand whether NaCl aerosols can act as a valid surrogate for coronavirus aerosols in filtration tests.

IMPLICATION

Our study is the first to demonstrate that electrospun air filters hold promise for providing efficient protection against airborne coronavirus particles. Cloth masks have been the most commonly used during the COVID-19 pandemic,[38] but our study along with previous research revealed their low filtration efficiency.[20,34] Therefore, wearing a surgical mask or other masks with an equal or a higher filtration efficiency should be encouraged. However, at the beginning of the pandemic, the mask/respirator shortage called for an urgent need to advance PPE. Meanwhile, it is highly desirable to develop innovative and efficient air filters for HVAC systems that can prevent the long-range transmission of coronavirus aerosols. Electrospinning is an economically feasible and industrially viable technology to fabricate highly efficient air filters,[39,40] and our study underscores its great potential for controlling the spread of coronavirus aerosols. With technology advancement and market growth, electrospun air filters will be highly competitive in comparison to meltblown masks/respirators and conventional HVAC air filters. More attractively, small-scale electrospinning apparatuses can provide a rapid response to the pandemic and produce highly tailorable filters with the desired performance for individuals and small communities.[41,42] By integration with additive manufacturing,[43] it is easy to design and fabricate customized masks, respirators, and HVAC air filters on the basis of the onsite needs.

ASSOCIATED CONTENT

Supporting Information

The Supporting Information is available free of charge at https://pubs.acs.org/doi/10.1021/acs.estlett.1c00337.

Filtration efficiency calculation and comparison, RNA extraction and RT-qPCR quantification, scheme of air filtration setup, ATR-FTIR characterization of polyelectrolyte coated filters, SEM of electrospun air filters, aerosol size distribution, and pore size distribution of air filters and face masks (PDF)

AUTHOR INFORMATION

Corresponding Authors

Danmeng Shuai − *Department of Civil and Environmental Engineering, The George Washington University, Washington, D.C. 20052, United States;* orcid.org/0000-0003-3817-4092; Phone: 202-994-0506; Email: danmengshuai@gwu.edu; Fax: 202-994-0127; http://materwatersus.weebly.com/

Yun Shen − *Department of Chemical and Environmental Engineering, University of California, Riverside, Riverside, California 92521, United States;* orcid.org/0000-0002-8225-1940; Phone: 951-827-2423; Email: yun.shen@ucr.edu; Fax: 951-827-5696; https://yunshen.weebly.com/

https://doi.org/10.1021/acs.estlett.1c00337
Environ. Sci. Technol. Lett. 2021, 8, 545−550

Authors

Hongchen Shen − *Department of Civil and Environmental Engineering, The George Washington University, Washington, D.C. 20052, United States*

Zhe Zhou − *Department of Civil and Environmental Engineering, The George Washington University, Washington, D.C. 20052, United States*

Haihuan Wang − *Department of Civil and Environmental Engineering, The George Washington University, Washington, D.C. 20052, United States; Department of Chemical and Environmental Engineering, University of California, Riverside, Riverside, California 92521, United States*

Mengyang Zhang − *Department of Civil and Environmental Engineering, The George Washington University, Washington, D.C. 20052, United States*

Minghao Han − *Department of Chemical and Environmental Engineering, University of California, Riverside, Riverside, California 92521, United States*

David P. Durkin − *Department of Chemistry, United States Naval Academy, Annapolis, Maryland 21402, United States;* orcid.org/0000-0001-5979-8449

Complete contact information is available at: https://pubs.acs.org/10.1021/acs.estlett.1c00337

Author Contributions

[‖]H.S., Z.Z., and H.W. contributed equally to the paper.

Notes

The authors declare no competing financial interest.

■ ACKNOWLEDGMENTS

We acknowledge NSF RAPID grants (CBET-2029411 and CBET-2029330) for supporting our research. We thank The George Washington University (GW) Nanofabrication and Imaging Center for SEM characterizations, GW BSL2+ laboratory facilities for the bioaerosol study, and the United States Naval Academy for ATR-FTIR characterizations. We thank Dominick J. Carluccio and Ryan Archer at the CH Technologies (USA), Inc., for characterizing the aerosol size distribution.

■ REFERENCES

(1) WHO Transmission of SARS-CoV-2: Implications for infection prevention precautions; https://www.who.int/news-room/commentaries/detail/transmission-of-sars-cov-2-implications-for-infection-prevention-precautions.

(2) Liu, Y.; Ning, Z.; Chen, Y.; Guo, M.; Liu, Y.; Gali, N. K.; Sun, L.; Duan, Y.; Cai, J.; Westerdahl, D.; et al. Aerodynamic analysis of SARS-CoV-2 in two Wuhan hospitals. *Nature* **2020**, *582*, 557−560.

(3) Van Doremalen, N.; Bushmaker, T.; Morris, D. H.; Holbrook, M. G.; Gamble, A.; Williamson, B. N.; Tamin, A.; Harcourt, J. L.; Thornburg, N. J.; Gerber, S. I.; et al. Aerosol and surface stability of SARS-CoV-2 as compared with SARS-CoV-1. *N. Engl. J. Med.* **2020**, *382* (16), 1564−1567.

(4) Konda, A.; Prakash, A.; Moss, G. A.; Schmoldt, M.; Grant, G. D.; Guha, S. Aerosol filtration efficiency of common fabrics used in respiratory cloth masks. *ACS Nano* **2020**, *14* (5), 6339−6347.

(5) Lu, J.; Gu, J.; Li, K.; Xu, C.; Su, W.; Lai, Z.; Zhou, D.; Yu, C.; Xu, B.; Yang, Z. COVID-19 outbreak associated with air conditioning in restaurant, Guangzhou, China, 2020. *Emerging Infect. Dis.* **2020**, *26* (7), 1628.

(6) Stephens, B.; Siegel, J. Ultrafine particle removal by residential heating, ventilating, and air-conditioning filters. *Indoor Air* **2013**, *23* (6), 488−497.

(7) Li, D.; Xia, Y. Electrospinning of nanofibers: Reinventing the wheel? *Adv. Mater.* **2004**, *16* (14), 1151−1170.

(8) Teo, W. E.; Ramakrishna, S. A review on electrospinning design and nanofibre assemblies. *Nanotechnology* **2006**, *17* (14), R89.

(9) Thavasi, V.; Singh, G.; Ramakrishna, S. Electrospun nanofibers in energy and environmental applications. *Energy Environ. Sci.* **2008**, *1* (2), 205−221.

(10) Dai, Y.; Liu, W.; Formo, E.; Sun, Y.; Xia, Y. Ceramic nanofibers fabricated by electrospinning and their applications in catalysis, environmental science, and energy technology. *Polym. Adv. Technol.* **2011**, *22*, 326−338.

(11) Dong, Z.; Kennedy, S. J.; Wu, Y. Electrospinning materials for energy-related applications and devices. *J. Power Sources* **2011**, *196* (11), 4886−4904.

(12) Qin, X.; Subianto, S., 17 - Electrospun nanofibers for filtration applications. In *Electrospun Nanofibers*; Afshari, M., Ed.; Woodhead Publishing: 2017; pp 449−466.

(13) Zhang, S.; Liu, H.; Tang, N.; Zhou, S.; Yu, J.; Ding, B. Spider-web-inspired PM0. 3 filters based on self-sustained electrostatic nanostructured networks. *Adv. Mater.* **2020**, *32*, 2002361.

(14) Gao, H.; He, W.; Zhao, Y.-B.; Opris, D. M.; Xu, G.; Wang, J. Electret mechanisms and kinetics of electrospun nanofiber membranes and lifetime in filtration applications in comparison with corona-charged membranes. *J. Membr. Sci.* **2020**, *600*, 117879.

(15) Matulevicius, J.; Kliucininkas, L.; Prasauskas, T.; Buivydiene, D.; Martuzevicius, D. The comparative study of aerosol filtration by electrospun polyamide, polyvinyl acetate, polyacrylonitrile and cellulose acetate nanofiber media. *J. Aerosol Sci.* **2016**, *92*, 27−37.

(16) Zhang, Q.; Welch, J.; Park, H.; Wu, C.-Y.; Sigmund, W.; Marijnissen, J. C. Improvement in nanofiber filtration by multiple thin layers of nanofiber mats. *J. Aerosol Sci.* **2010**, *41* (2), 230−236.

(17) Liu, Y.; Park, M.; Ding, B.; Kim, J.; El-Newehy, M.; Al-Deyab, S. S.; Kim, H.-Y. Facile electrospun polyacrylonitrile/poly (acrylic acid) nanofibrous membranes for high efficiency particulate air filtration. *Fibers Polym.* **2015**, *16* (3), 629−633.

(18) Leung, W. W. F.; Sun, Q. Electrostatic charged nanofiber filter for filtering airborne novel coronavirus (COVID-19) and nano-aerosols. *Sep. Purif. Technol.* **2020**, *250*, 116886.

(19) Choi, J.; Yang, B. J.; Bae, G.-N.; Jung, J. H. Herbal extract incorporated nanofiber fabricated by an electrospinning technique and its application to antimicrobial air filtration. *ACS Appl. Mater. Interfaces* **2015**, *7* (45), 25313−25320.

(20) Whiley, H.; Keerthirathne, T. P.; Nisar, M. A.; White, M. A.; Ross, K. E. Viral Filtration Efficiency of Fabric Masks Compared with Surgical and N95 Masks. *Pathogens* **2020**, *9* (9), 762.

(21) Rengasamy, S.; Shaffer, R.; Williams, B.; Smit, S. A comparison of facemask and respirator filtration test methods. *J. Occup. Environ. Hyg.* **2017**, *14* (2), 92−103.

(22) Bárcena, M.; Oostergetel, G. T.; Bartelink, W.; Faas, F. G.; Verkleij, A.; Rottier, P. J.; Koster, A. J.; Bosch, B. J. Cryo-electron tomography of mouse hepatitis virus: insights into the structure of the coronavirion. *Proc. Natl. Acad. Sci. U. S. A.* **2009**, *106* (2), 582−587.

(23) Ye, T.; Durkin, D. P.; Hu, M.; Wang, X.; Banek, N. A.; Wagner, M. J.; Shuai, D. Enhancement of nitrite reduction kinetics on electrospun Pd-carbon nanomaterial catalysts for water purification. *ACS Appl. Mater. Interfaces* **2016**, *8* (28), 17739−17744.

(24) Bingöl, B.; Meyer, W. H.; Wagner, M.; Wegner, G. Synthesis, microstructure, and acidity of poly(vinylphosphonic acid). *Macromol. Rapid Commun.* **2006**, *27*, 1719−1724.

(25) Ghosh, S.; Dellibovi-Ragheb, T. A.; Kerviel, A.; Pak, E.; Qiu, Q.; Fisher, M.; Takvorian, P. M.; Bleck, C.; Hsu, V. W.; Fehr, A. R.; Perlman, S.; Achar, S. R.; Straus, M. R.; Whittaker, G. R.; de Haan, C. A. M.; Kehrl, J.; Altan-Bonnet, G.; Altan-Bonnet, N. *β*-Coronaviruses use lysosomes for egress instead of the biosynthetic secretory pathway. *Cell* **2020**, *183* (6), 1520−1535.e14.

(26) Jayaraman, S.; Song, Y.; Vetrivel, L.; Shankar, L.; Verkman, A. Noninvasive in vivo fluorescence measurement of airway-surface liquid depth, salt concentration, and pH. *J. Clin. Invest.* **2001**, *107* (3), 317−324.

(27) Ramalingam, K.; Mujib, A.; Sarkar, A.; Sethuraman, S.; Bastian; Kallapur, B. Quantitative estimation of sodium, potassium and total protein in saliva of diabetic smokers and nonsmokers: A novel study. *J. Nat. Sc. Biol. Med.* **2013**, *4* (2), 341.
(28) Ahmed, W.; Bertsch, P.; Bivins, A.; Bibby, K.; Farkas, K.; Gathercole, A.; Haramoto, E.; Gyawali, P.; Korajkic, A.; McMinn, B. R.; et al. Comparison of virus concentration methods for the RT-qPCR-based recovery of murine hepatitis virus, a surrogate for SARS-CoV-2 from untreated wastewater. *Sci. Total Environ.* **2020**, *739*, 139960.
(29) Soliman, S.; Sant, S.; Nichol, J. W.; Khabiry, M.; Traversa, E.; Khademhosseini, A. Controlling the porosity of fibrous scaffolds by modulating the fiber diameter and packing density. *J. Biomed. Mater. Res., Part A* **2011**, *96A* (3), 566−574.
(30) Zuo, F.; Zhang, S.; Liu, H.; Fong, H.; Yin, X.; Yu, J.; Ding, B. Free-standing polyurethane nanofiber/nets air filters for effective PM capture. *Small* **2017**, *13* (46), 1702139.
(31) Chen, N.; Zhou, M.; Dong, X.; Qu, J.; Gong, F.; Han, Y.; Qiu, Y.; Wang, J.; Liu, Y.; Wei, Y.; et al. Epidemiological and clinical characteristics of 99 cases of 2019 novel coronavirus pneumonia in Wuhan, China: a descriptive study. *Lancet* **2020**, *395* (10223), 507−513.
(32) Podgorski, A.; Bałazy, A.; Gradoń, L. Application of nanofibers to improve the filtration efficiency of the most penetrating aerosol particles in fibrous filters. *Chem. Eng. Sci.* **2006**, *61* (20), 6804−6815.
(33) He, X.; Reponen, T.; McKay, R. T.; Grinshpun, S. A. Effect of particle size on the performance of an N95 filtering facepiece respirator and a surgical mask at various breathing conditions. *Aerosol Sci. Technol.* **2013**, *47* (11), 1180−1187.
(34) Hill, W. C.; Hull, M. S.; MacCuspie, R. I. Testing of commercial masks and respirators and cotton mask insert materials using SARS-CoV-2 virion-sized particulates: comparison of ideal aerosol filtration efficiency versus fitted filtration efficiency. *Nano Lett.* **2020**, *20* (10), 7642−7647.
(35) Mueller, A. V.; Fernandez, L. A. Assessment of Fabric Masks as Alternatives to Standard Surgical Masks in Terms of Particle Filtration Efficiency. *medRxiv* **2020**.
(36) Zangmeister, C. D.; Radney, J. G.; Vicenzi, E. P.; Weaver, J. L. Filtration efficiencies of nanoscale aerosol by cloth mask materials used to slow the spread of SARS-CoV-2. *ACS Nano* **2020**, *14* (7), 9188−9200.
(37) Leung, W. W.-F.; Sun, Q. Charged PVDF multilayer nanofiber filter in filtering simulated airborne novel coronavirus (COVID-19) using ambient nano-aerosols. *Sep. Purif. Technol.* **2020**, *245*, 116887.
(38) Chauhan, P.; Hellstrom, S.; Hughes, J.; Rothenberg, J. *Survey: In the US, people say their use of masks may endure*; https://www.mckinsey.com/featured-insights/americas/survey-in-the-us-people-say-their-use-of-masks-may-endure (12/24/2020).
(39) Yu, M.; Dong, R. H.; Yan, X.; Yu, G. F.; You, M. H.; Ning, X.; Long, Y. Z. Recent advances in needleless electrospinning of ultrathin fibers: from academia to industrial production. *Macromol. Mater. Eng.* **2017**, *302* (7), 1700002.
(40) Persano, L.; Camposeo, A.; Tekmen, C.; Pisignano, D. Industrial upscaling of electrospinning and applications of polymer nanofibers: A review. *Macromol. Mater. Eng.* **2013**, *298* (5), 504−520.
(41) Xu, S.-C.; Qin, C.-C.; Yu, M.; Dong, R.-H.; Yan, X.; Zhao, H.; Han, W.-P.; Zhang, H.-D.; Long, Y.-Z. A battery-operated portable handheld electrospinning apparatus. *Nanoscale* **2015**, *7* (29), 12351−12355.
(42) Yan, X.; Yu, M.; Ramakrishna, S.; Russell, S. J.; Long, Y.-Z. Advances in portable electrospinning devices for in situ delivery of personalized wound care. *Nanoscale* **2019**, *11* (41), 19166−19178.
(43) Choong, Y. Y. C.; Tan, H. W.; Patel, D. C.; Choong, W. T. N.; Chen, C.-H.; Low, H. Y.; Tan, M. J.; Patel, C. D.; Chua, C. K. The global rise of 3D printing during the COVID-19 pandemic. *Nat. Rev. Mater.* **2020**, *5* (9), 637−639.

https://doi.org/10.1021/acs.estlett.1c00337
Environ. Sci. Technol. Lett. 2021, 8, 545−550